Int. J. Econ. Environ. Geol. Vol. 15 (2) 32-42, 2024
Journal home page: www.econ-environ-geol.org

Open Access
ISSN: 2223-957X

Hydrocarbon Potential Evaluation of Sandstone Reservoirs in Lower Goru Formation Miano Gas Field in Middle Indus Basin, Sindh, Pakistan

Saeed Ahmed, *Sadaf Naseem

Department of Geology, University of Karachi, Pakistan

*Email: snaseem@uok.edu.pk

Abstract: The Middle Indus basin (MIB) is a potential hydrocarbon sedimentary basin of Pakistan. This study was carried out to interpret the petrophysical well log data of Minao gas field of three wells (Miano-1, 2 and 3) to characterize the Lower Goru reservoir. Indonesian model was applied to estimate the in-situ water saturation Sw of the Lower Goru reservoir. Contour maps were used to understand the lateral and vertical variation in reservoir characteristics. In addition, M-N lithology cross plots were also used to interpret the lithological heterogeneity and homogeneity within the reservoir. There were four sand units recognized as Sand A, B, C and D within Lower Goru reservoir based on the estimation of effective porosity (Φeff), permeability (K), shale volume (Vsh), water saturation (Sw) and hydrocarbon saturation (Shc). The Sand B showed good potential for hydrocarbon as indicated by shale volume Vsh (10 to 14%), effective porosity Φeff (19 to 22%), permeability K (798 to 847 mD), water saturation Sw (19 to 22%) and hydrocarbon saturation Shc (77 to 80%). Data revealed that in north and northeast side, there is an increase in reservoir quality and thickness, while it decreased in south to southwest side. Shale volume decreased in north to northeast with low water saturation and high hydrocarbon saturation. Results reveal that north to northeast direction of Miano gas field is ideal for the hydrocarbon recovery. More exploratory wells are recommended to be drilled in this direction to maximize the hydrocarbon production from the Lower Goru reservoir.

Keywords: Indus Basin, Goru Formation, petrophysical evaluation, hydrocarbon potential, Pakistan.

Introduction

Among various reservoir evaluation techniques, petrophysical well logging is a proven and the most beneficial method used worldwide for reservoir characterization (Cosentino and Cheadle, 2001). Petrophysical well logging involves to evaluate the efficiency and performance of reservoir rocks using various parameters to estimate the commercially recoverable hydrocarbons. This approach is used to assess the capability of reservoir to store and transmit hydrocarbons, and is highly useful for calculating pay zone and volume of hydrocarbon reserves (Asquith and Gibsen, 1982). The essential petrophysical parameters included effective porosity, permeability and fluid saturation (Alabi and Sedara, 2016). Numerous studies have been carried out to investigate the petrophysical characteristics of Lower Goru Formation of Cretaceous age for its hydrocarbon prospects evaluation (Ashraf et al., 2016; Anees et al., 2019; Abbas et al., 2019). In present study petrophysical logging data, including effective porosity Φeff, permeability K, shale volume Vsh, water saturation Sw and type of in-situ fluids were used to evaluate Lower Goru reservoir in Miano gas field for its petroleum potential. The Miano gas and condensate field is located in Middle Indus Basin (MIB), Khairpur district of Sindh province, Pakistan (Khan et al., 2013). Study area lies between longitudes 69˚12'E and 69˚28'E and latitudes 27˚14'N and 27˚32'N, respectively (Fig. 1).

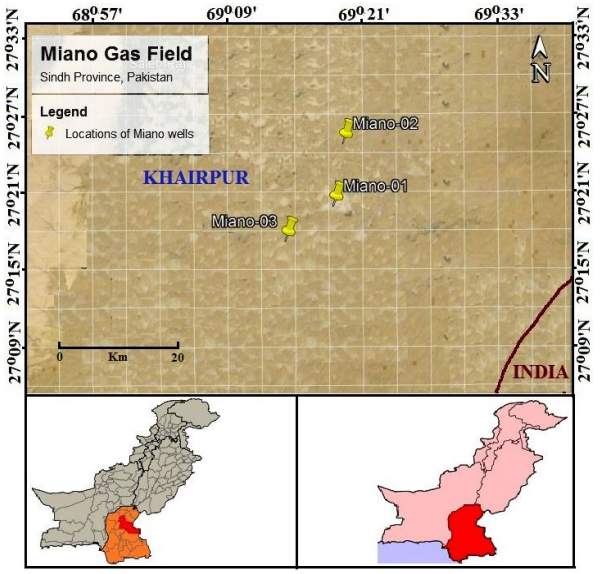

Fig.1 Location map of Miano-1, 2 and 3 wells.

It is bounded by Indian shield in the east and the Kirthar Fold Belt in the west. Tectonically, the area is located in the Middle Indus Basin (MIB) along the western margin of the Indian Plate, and surrounded by Mari-Kandhkot High in NE and the Jacobabad-Khairpur High

in the south-west. The study area is mainly covered by Recent to Sub-Recent alluvium, while subsurface rocks ranged in age from Permian to Mesozoic. The reservoir in the Miano-2 well is configured with a structural trap developed as a result of horst and graben and roll-over anticlinal structures. The well Miano-2 was drilled in a horst which is bounded by two normal faults (Ahmed et al., 2013).

Middle Indus Basin (MIB) is one of the hydrocarbon prone basins and several studies indicated that it contains 70% of Pakistan's known gas reserves (Raza and Ahmed, 1990; Ahmed et al., 2013). Petroleum system of Miano area is comprised of Lower Cretaceous aged Sembar Formation as a source rock, which contains black shale with 0.5-3.5% TOC, while A, B, C, and D units of Lower Goru sandstone act as a reservoir and Upper Goru shale and marl as a seal rock. The first Miano-1 exploratory well was drilled in 1992. Gas was discovered in 8 m thick sandstone B unit, part of Cretaceous aged Lower Goru reservoir with 35.3 MMcf/D flow rate (Krois et al., 1998). The B Sand of Lower Goru is widely spread in Middle Indus Basin (MIB) and shows extreme heterogeneities both vertically and laterally. Therefore, it is necessary to distinguish between shale and other rocks through various well log responses, including density porosity, neutron porosity, sonic transit time, water conductivity, natural radioactivity and shale resistivity.

The objective of this study is to estimate the major characteristics of reservoir for better understanding of hydrocarbon production capacity of Lower Goru for recoverable hydrocarbons.

This study will contribute to better understanding and predicting the subsurface structures, petroleum play and the hydrocarbon-bearing zones in highly heterogeneous Lower Goru reservoirs in the region of Middle Indus Basin (MIB). Indus basin is classified as Extra continental Trough Downwarp, it is elongated in shape and oriented in NE-SW direction. Its eastern part is comprised of platform, which dips gently and monoclinically towards NW. The Indus basin got bent and twisted under the influence of plate collision in Early Tertiary period and resulted in Upper, Middle and Lower sub-basins (Powell et al., 1979). The Upper and Lower Indus basins are oil prone, while Middle Indus Basin (MIB) is recognized as gas prone. The Middle Indus Basin (MIB) contains major hydrocarbon reserves and it has been extensively explored by several oil and gas companies. Study area is situated in NE to SE of Middle Indus Basin. In the eastern side, it is surrounded by Indian Shield and Sulaiman Fold Belt in the west, Sargodha High in the north while Jacobabad/Khairpur High in the south. The tectonic setting of the area is characterized by Gondwanian and Tethyan domain. Jurassic rifting, breakup of Gondwana super continent, Early Cretaceous northward Indian plate drift (15 to 20 cm/yr) from Africa, counter clock wise movement (55 to 50 Ma) and collision of Indian plate with Eurasian plate initiated the intense episodic deformation in the west of the Lower and Middle Indus Basin (Qadri, 1995). Massive Cenozoic plate convergence with Tethyan and Eurasian plates produced complex thrust and wrench geometries in the rocks of the northern and western parts of Indian plate. Similarly, intensive tectonics stresses developed from south to north of the study area leading to the formation of regional Jacobabad/Khairpur High, Lower Indus Trough, normal faults and NNW–SSE trending thick-skinned wrenching. Significant unconformities were developed in Indus Basin and its eastern parts (Powell et al., 1979). Tertiary strata have direct contact with Jurassic sequence, which is also dissected by Eocene/Oligocene deep rooted and shallow wrench faults. The collision of Indian and Eurasian plates has greatly affected the study area, and northwest to southeast trending parallel or sub-parallel oblique pattern strike slip faults and SE–NW trending fractures have dissected the Miano area. These structures provided an ideal condition for the development of structural traps. The Miano area is situated in Indus trough area (Raza and Ahmed, 1990; Krois et al., 1998; Ahmed et al., 2013)

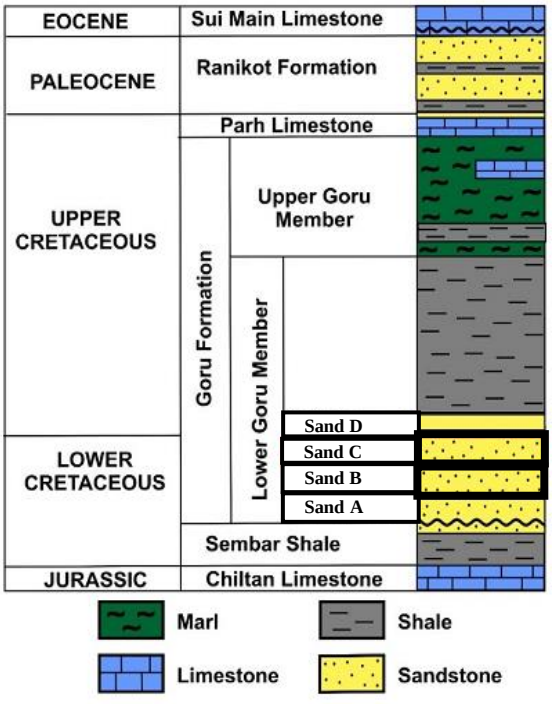

Fig. 2 Stratigraphy of Middle Indus Basin (Modified after Ahmed et al., 2004, Krois et al., 1998).

The black shale of Sembar Formation (Early Cretaceous) is the main source rock for the petroleum system of the basin (Fig. 2). In Middle and Lower Indus Basins, its thickness varied between 0-260 m, while its depth increases towards the western side of the basin. The Sembar Formation is the lowermost unit of the Cretaceous strata, which directly overlies the Chiltan Limestone of Middle Jurassic age and shows thinning towards the east (Kadri, 1995). The Sembar Formation is correlated with the Chichali Formation of Upper Indus Basin. The Sembar is mainly composed of clastic rocks, shales, sandstones and siltstone. Characteristically the formation, in the outcrop consists of black silty shale with glauconite (Qadri, 1995). The maximum thickness (>1000m) of the Sembar Formation (source rock) is found in Sulaiman Lobe area. Sembar Formation contains type-III kerogen and has shown gas generation potential. High (5.0°C per 100m) geothermal gradient has significantly raised the thermal maturity of Sembar Formation and therefore, it is mainly over mature (as indicated by > 1.35% vitrinite reflectance R° value) which increases from eastern to western side of the basin (Wandrey et al., 2004).

The Goru Formation is widely distributed both in the Kirthar and Sulaiman provinces. Regionally the thickness increases towards the center of the Karachi Embayment. In the Kirther Fold Belt, the Goru Formation thins gradually towards north. In the western margin, the formation is absent, mainly because of erosion (Qadri, 1995). The Goru Formation is correlated with the Lumshiwal Formation in Upper Indus Basin (Shah, 1980). On the basis of lithological content it has been divided into Lower Goru, and Upper Goru (Qadri, 1995). The thickest Goru sedimentation occurs within the Karachi Embayment.

The Goru Formation of Late Cretaceous age was deposited in a shallow marine and estuarine environment as indicated by presence of oyster and pelecypod fossils. On the basis of lithology, it is mainly categorized into Upper and Lower units (Fig.2). The Upper Goru unit is chiefly composed of shale and marl, which act as a seal rock (Kazmi and Jan, 1997) The upper section of the Lower Goru Formation reveals as stratigraphical seal, which is generally composed of transgressive, siderite cemented shales and siltstones. It is cemented by chlorite and comprises almost 80% of the clay fraction. This considerable amount of the chlorite has decreased the porosity of the rocks (McPhee and Enzendorfer, 2004).

The lower section is generally composed of medium to coarse grained sandstone. Lithological characteristics of Lower Goru sandstone make it an excellent reservoir rock in the Middle Indus Basin (Qadri, 1995). The lower part of Lower Goru Formation is further divided (from bottom to top) into four stratigraphic intervals recognized as sand units A, B, C, and D. (Krois et al., 1998). The sand units A and B proved as potential gas reservoirs, while C and D exhibited low productive sand units (Ahmad et al., 2004). Petrographic analysis proved that the A and B units are composed of quartz arenite, whereas the C unit is sublithic to lithic arenite, which includes a considerable amount (approximately 13%) of moderately altered basic volcanic rock particles (McPhee and Enzendorfer, 2004, Berger et al., 2009).

Materials and Methods

The petrophysical well log data of Miano-1, Miano-2 and Miano-3 wells were used for this study to evaluate the hydrocarbon potential of Lower Goru reservoir of Miano gas field (Fig. 3). A set of petrophysical well logs (CAL, SP, GR, NGS, LLD, DT, NPHI, DROH) were used for the estimation of reservoir parameters such as porosity, permeability, shale volume Vsh and water saturation Sw. Geological structure and depositional environment were also interpreted from the well log data.

The study was carried out to recognize and distinguish potential sand units within Lower Goru sand by GR and SP lithology logs. Furthermore, DT, NPHI, and DRHO logs were also used to estimate the effective porosity and types of pore-fluids. Shale volume was estimated by GR logs, while SP and LLD logs were used to determine the reservoir boundaries and hydrocarbon indication within the reservoir. Water saturation Sw was estimated by two equations of Archie and Indonesian and was generalized for water saturation (Archie, 1942). Petrophysical well log data was also used to derive formulas, equations and log units for water saturation Sw, effective porosity Φ, hydrocarbon saturation Shc and volume of shale Vsh. Permeability was calculated by standard methods (Wyllie et al., 1956; Timur, 1968; Coates and Dumanoir, 1974).

Resistivity of water (Rw) of in-situ fluid was determined by formation temperature, NaCl concentration (Patzek et al., 2000) and log interpretation chart book (Schlumberger, 1989). On the basis of wellbore temperature of the Miano wells, the formation temperature gradient (m/^{o}F) of bottom hole was correlated with the data of nearby Kadanwari gas field. Resistivity of in-situ formation water (Rw) was used to estimate the value of water saturation (S_w) and hydrocarbon saturation (Shc) of the Sand (A to D) of Lower Goru reservoir. Cross-plots of porosity logs for in-situ saturated fluid were used to obtain information about vertical distribution of hydrocarbon and type of fluids trapped into the reservoir rock. The log ASCII standard (LAS) files of petrophysical well logs of three

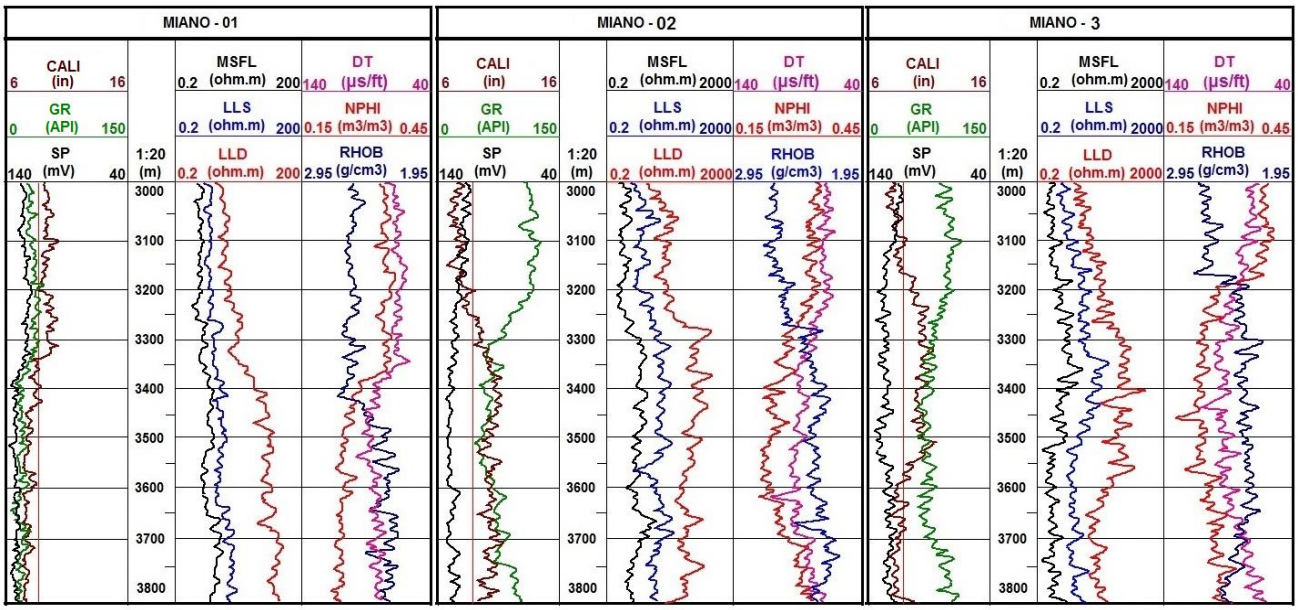

Fig.3 Petrophysical logs of Miano-1, 2 and 3 wells.

Miano wells (1, 2 & 3) were acquired from Directorate General of Petroleum Concession (DGPC) and Land Mark Resources (LMKR). The LAS data was used to plot Miano-1, Miano-2 and Miano-3 log curves using Techlog® and LogPlot® (Fig. 3). These softwares were also used to construct the stratigraphic columns and well correlations. Surfer® was used to plot contour maps.

Shale Volume

Gamma ray GR log was used to determine the shale intercalation and to calculate the volume of shale in reservoir rock by using Asquith and Gibson (1982) linear relationship as follows:

$$GR_{index} = \frac{GR_{\log} - GR_{\min}}{GR_{\max} - GR_{\min}}$$

Corrected volume of shale is estimated by Lorinovo (1969) is given below.

$$\mathrm{Vsh} = 0.083 \times \left(2^{(3.7 \times \mathrm{GR_{index}})^{-1}}\right)$$

Density Porosity

Porosity of the reservoir was estimated from the equation, used by density log (Whiteman, 1982; Asquith et al., 2004). The density log porosity acquired directly from log without correction for clay content is considered as total porosity (Cai et al., 2017). It is calculated by using the following formula (Schlumberger, 1989).

$$\varnothing_{\mathrm{d}} = \frac{\rho \mathrm{m} - \rho \mathrm{b}}{\rho \mathrm{ma} - \rho \mathrm{fl}}$$

Effective porosity Φeff is estimated by the density porosity Φd and corrected shale volume.

$$\varnothing_{\mathbf{eff}} = \cdot \varnothing_{\mathrm{d}} \times (1 - V_{sh})$$

Sonic Porosity

Neutron and sonic logs were used for the calculation of total and effective porosity. The corrected sonic density was estimated by Wyllie et al. (1956) expression, which is used for consolidated and compacted formations. A correction factor is necessary to apply for poorly consolidated or unconsolidated rocks.

$$\phi_s = \frac{\Delta t - \Delta t_{\mathrm{ma}}}{\Delta t_f - \Delta t_{\mathrm{ma}}} \times \frac{1}{C_p}$$

Where the compaction correction factor C_p is;

$$C_p = \frac{\Delta t_{\mathrm{sh}}(C)}{100}$$

Permeability

Three empirical models were utilized in the study for permeability estimation. All of these models were derived from the correlation among permeability, porosity and water saturation. Permeability was estimated by Timur (1968), and Wyllie and Rose (1950) equations.

Wyllie and Rose (1950) framework and equation:

$$K^{1/2} = 250 \times \emptyset^3 / S_{w\,irr} \text{ (medium gravity oils)}$$

$$K^{1/2} = 79 \times \emptyset^3 / S_{w\,irr} \text{ (dry gas)}$$

$$K = \left(250 * \frac{\Phi_{eff}^{3}}{Swir}\right)^2$$

Permeability from calculated porosity and water saturation of the reservoir by Timur (1968) model are as follows.

$$K = \left(\frac{93\, x\, \phi^{2.2}}{S_{wirr}}\right)^2 \qquad K = 0.136 \frac{\phi^{4.4}}{S_{wirr}^{\ 2}}$$

Permeability from calculated porosity and water saturation of the reservoir by Coates and Dumanoir (1974) model is:

$$K^{½} = 100 \frac{\phi^2 (1 - S_{wirr})}{S_{wirr}}$$

Saturation of Water

Water saturation was calculated using Archie (1942) model.

$$S_w = \left(\frac{F.R_w}{R_t}\right)^{1/n}$$

Where F is formation factor estimated by

$$F = \frac{1}{\Phi^2}$$

Rw is water resistivity estimated by formation temperature and NaCl concentration, Rt is true formation resistivity estimated by micro short focused log MSFL, where n is a cementation factor for moderately shaley sand with 1.8 value.

Water saturation of Leveaux and Poupon (1971) expressed the mathematical model known as the Indonesian equation to estimate the water saturation.

The theory was derived from freshwater properties and maximum amount of shale encountered in several Indonesian oil reservoirs. The mathematical expression can be described as:

$$S_w = \left\{ R_t \left[\left(\frac{V_{sh}^{2-V_{sh}}}{R_{sh}} \right)^{\frac{1}{2}} + \left(\frac{\phi_e^m}{R_w} \right)^{\frac{1}{2}} \right] \right\}^{-\frac{1}{n}}$$

Saturation of Hydrocarbon

Water saturation was calculated to estimate the hydrocarbon saturation (Shc), the subsequent Shepherd (2009) relation is used.

Results and Discussion

A petrophysical well log analysis is an important tool to estimate the physical and chemical properties of reservoir and in-situ fluids. A systematic qualitative and quantitative approach was used for well logs interpretation, estimation of reservoir and recoverable hydrocarbon from Lower Goru reservoir. Petrophysical well log data of Miano-1, Miano-2 and Miano-3 was used to understand the petroleum play system and characterization of Lower Goru reservoir of Cretaceous age (Fig.3). On the basis of petrophysical and lithological characteristics, Lower Goru reservoir is divided into four sand units including Sand A, B, C and D within the reservoir (Jiang et al., 2021; Anees et al., 2022).

In Miano-1 well the Sand-A was found between 3740 - 3825m interval and the shale volume was estimated up to 11.4%, effective porosity 17.2%, permeability 633.3mD, water saturation 18.3%, and hydrocarbon saturation was 81.7% (Fig. 4, Table 1). In addition Sand-B was encountered between 3235 to 3740m interval and its shale volume was estimated up to 10.3%, effective porosity 22.5%, permeability 847.8mD, water saturation 22.4% and hydrocarbon saturation was 77.6%. Sand-C was encountered at the depth of 3195 to 3235m interval, its shale volume is estimated up to 18.7%, effective porosity 8.1%, permeability 56.2mD, water saturation 68.1% and hydrocarbon saturation 31.9%. Sand-D was found at the depth interval of 3160m to 3195m. The shale volume is estimated around 20.6%, effective porosity 7.8%, permeability 18.4mD, water saturation 88.7% and hydrocarbon saturation was 11.3%. In Miano-2 well Sand-B was found between 3380m-3548m interval, shale volume was 12.8%, effective porosity 20.3%, permeability 833.1mD, water saturation 21.3% and hydrocarbon saturation was 78.7%.

Sand-C was marked at the of depth 3300m to 3380m, shale volume was estimated 15.3%, effective porosity 9.1%, permeability 59.8mD, water saturation 61.7% and hydrocarbon saturation was 38.3%. Whereas, Sand-D was encountered at the depth of 3135 to 3300m interval, shale volume was 19.1%, effective porosity 8.8%, permeability 21.3mD, water saturation 82.9% and hydrocarbon saturation 17.1% (Fig. 4, Table 1).

Similarly in Miano-3 well, Sand-B was marked at the depth of 3160 to 3448m interval, shale volume was 14.2%, effective porosity 19.5%, permeability 798.6mD, water saturation 19.4% and hydrocarbon saturation was 80.6%. In addition, Sand-C was found at the interval of 3080m to 3160m, shale volume was 17.9%, effective porosity 7.8%, permeability 48.7mD, water saturation 59.9% and hydrocarbon saturation was 40.1% Whereas, Sand-D was found between 2985m-3080m interval, shale volume was 21.6%, effective porosity 6.3%, permeability 28.2mD, water saturation 89.3% and hydrocarbon saturation was 10.7%. The value of effective porosity is promising in Sand-B, while it shows low water saturation and high hydrocarbon saturation. Shale volume was increasing in Sand-C and D of all three Miano wells. Effective porosity and permeability were reducing from Sand-C to D, while increasing water and decreasing hydrocarbon saturation trend is noted within Sand-C and D (Fig. 4).

Table 1. Estimated petrophysical parameters of Lower Goru reservoir.

Well	Unit	Interval (m)	Vsh (%)	Φeff (%)	K (mD)	Sw (%)	Shc (%)
M-03	D	2985-3080	21.60	06.30	28.20	89.30	10.70
M-03	C	3080-3160	17.90	07.80	48.70	59.90	40.10
M-03	B	3160-3448	14.20	19.50	798.60	19.40	80.60
M-02	D	3135-3300	19.10	08.80	21.30	82.90	17.10
M-02	C	3300-3380	15.30	09.10	59.80	61.70	38.30
M-02	B	3380-3548	12.80	20.30	833.10	21.30	78.70
M-01	D	3160-3195	20.60	07.80	18.40	88.70	11.30
M-01	C	3195-3235	18.70	08.10	56.20	68.10	31.90
M-01	B	3235-3740	10.30	22.50	847.80	22.40	77.60
M-01	A	3740-3825	11.40	17.20	633.30	18.30	81.70

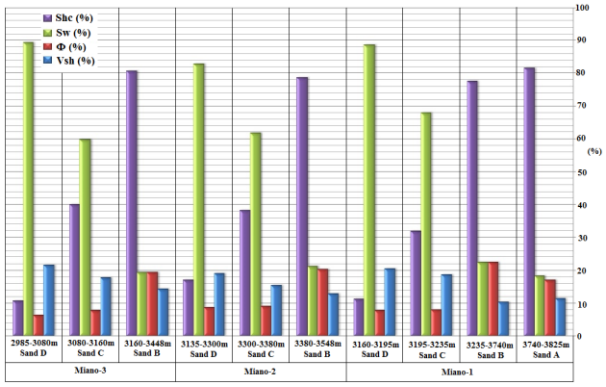

Fig. 4 Comparison of petro physical parameters of Lower Goru Sand units

Shale volume is an essential tool to differentiate between clean homogenous and heterogeneous sand. The gamma ray GR log was applied to estimate the volume of shale distribution. The higher value of gamma ray GR log is a marker of dense shale and lower

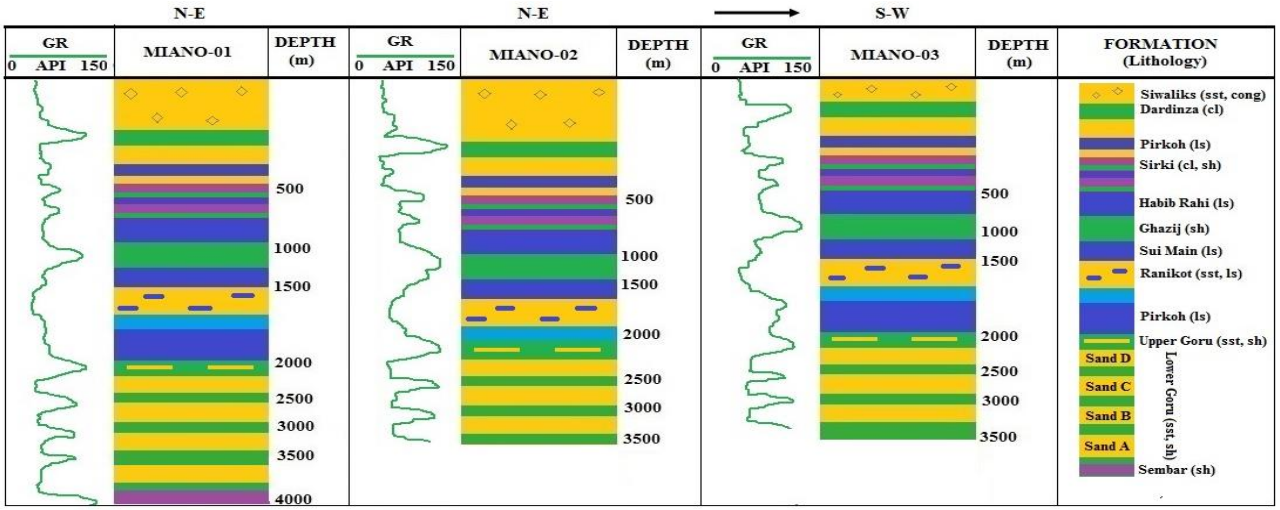

Fig. 5 Gamma Ray (GR) log response in Miano-1, 2 and 3 wells.

value shows the clean sand. Interpretation of natural gamma ray spectral (NGS) log shows the high concentration of thorium rich radioactive heavy minerals, which indicate the presence of sand intercalations within the reservoir (Fig. 5, 6). Shale volume is relatively low in Sand-B in all three Miano wells. Presence of shale and sand intercalations confirms that Goru Formation was deposited in fluvio-deltaic environment.

Fig. 6 Intercalation of clay and sand profile in Lower Goru reservoir of Miano wells.

Hydrocarbon Saturation of Pay Zone

Saturation of hydrocarbon (Shc) was estimated for Sand A to D within the Lower Goru reservoir in all three Miano wells. Resistivity logs of MSFL, ILD, and LLD showed the presence of hydrocarbon bearing zones. On the basis of estimated hydrocarbon saturation in Miano-1, 2 and 3 wells there were four different sand units recognized as Sand A, Sand B, Sand C and Sand D within the Lower Goru reservoir. Hydrocarbon saturation of each sand within Lower Goru reservoir is displayed in Table 1. There are ten different sand data sets as Sand A, Sand B, Sand C and Sand D used for each Miano well (Fig. 6). Distinctly Sand B of Miano-1 well at depth of 3235 to 3740m interval has low water saturation (22.4%) and good (77.6%) hydrocarbon saturation. Sand B of Miano-2 well at the depth of 3380 to 3548m interval has low (21.3%) water saturation and (78.7%) good hydrocarbon saturation.

Sand-B of Miano-3 well at the depth of 3160 to 3448m interval has low water saturation (19.4%) and good (80.6%) hydrocarbon saturation, respectively.

It was observed that the water saturation is lower than 25% in Sand B of all three Miano wells. Therefore, Sand B proved to be rich in hydrocarbon with about 80% good reservoir qualities. While, Sand C and Sand D show high water saturation (60% to 80%) containing low hydrocarbon (20% to 40%), and considered to be less hydrocarbon prone sand units of Lower Goru reservoir.

Lateral Variation in Reservoir Characteristics

In order to evaluate the lateral variation, lithology logs were constructed and used to correlate Miano wells. Contour maps were also used to understand the shale distribution within the reservoir. The contour map of shale volume indicated that the shale content ranged between 10%-21% (Fig. 7). Lower value of shale 10% to 14% was found within Sand- A and B while a higher value of 21% was encountered in C and D sands. It also revealed that shale volume reduced in north and southwestern side, while it increased towards the south to south-east of the study area. Effective porosity map showed the distribution of effective porosity values, which are decreasing from 6% to 9% in Sand C and D, while there is an increased trend of 19% to 22% within Sand A and B (Fig. 8). Effective porosity distribution showed the pattern of high value in northeastern and

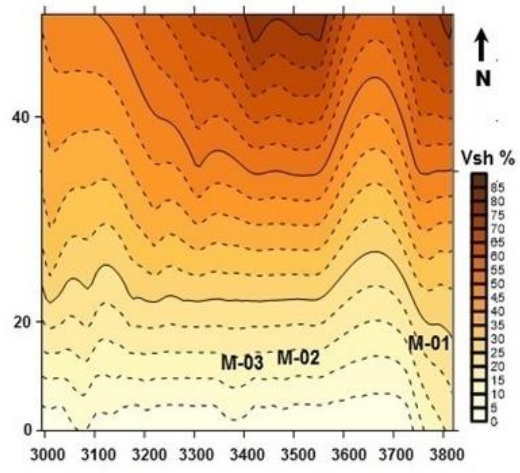

Fig. 7 Volume of shale distribution in Lower Goru Reservoir of Miano wells.

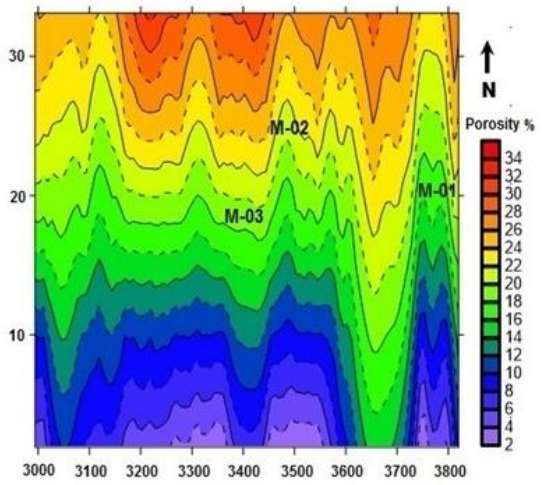

Fig. 8 Effective porosity distribution in Lower Goru Reservoir of Miano wells.

low values in southeastern, and western sides. Porosity distribution might be influenced by early diagenetic

process and presence of chloritic clays, and heavy minerals as cements growth has played a significant role to reduce the porosity (Krois et al., 1998). In addition, the Lower Goru reservoir is overlain by thick sedimentary sequence of Siwaliks and Ranikot Group (Eocene). As a result, overburden and compaction has significantly reduced the porosity of reservoir **(**Ahmed et al., 2013).

Permeability map shows the permeability distribution values between 633mD to 847mD within Sand A and B, and minimum 18mD to 59mD within Sand C and D (Fig. 9). The value of permeability increases in northeastern parts, while decreasing in southeastern to western side. Water saturation map reveals that minimum water saturation ranges between 18% to 22% within Sand A and B, while its maximum values between 59%-89% are found within Sand C and D (Fig. 10). High values of water saturation were found in north and southeastern parts, while lower values were found in northeastern area. Furthermore, hydrocarbon saturation map shows the higher saturation values of 77% to 81% are found within Sand A and B, while lower values (10% to 40%) occur within Sand C and D (Fig. 11).

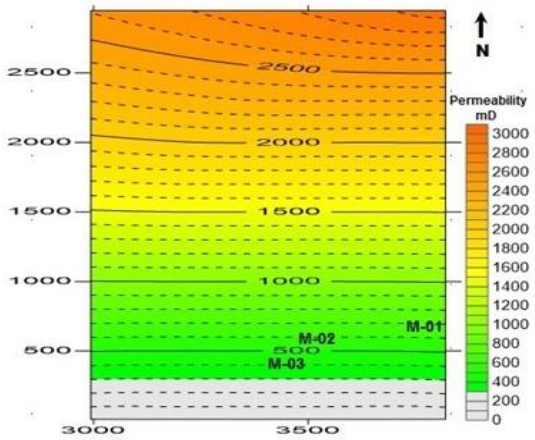

Fig. 9 Permeability distribution in Lower Goru Reservoir of Miano wells.

Well to well correlation among three wells (Miano-1, 2 and 3) interpreted by GR log. Gamma ray (GR) log represents the true lithology profile of all three Miano wells which indicates the lateral variation in lithology and demarcates the top of each lithological unit (Fig. 5, 6). Gamma ray (GR) log shows intercalation of clay within sand A to D into the Lower Goru reservoir. Thickness of Lower Goru reservoir increased in north to north eastern side of study area indicating high potential of hydrocarbon accumulation. The net pay thickness of the Lower Goru reservoir increased from southwestern part to north and northeastern side. Study reveals that Sand B is the most prolific zone within the Lower Goru reservoir and south to southeastern part of the area is gas prone.

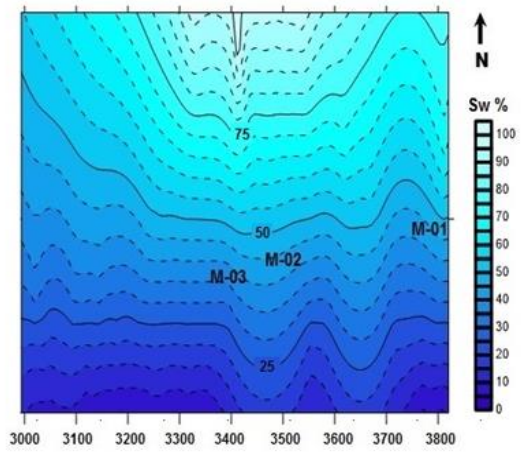

Fig. 10 Water saturation distribution in Lower Goru Reservoir of Miano wells.

The cross-plot of M-N is a tool to define multi mineral mixtures lithology by a neutron, density, and sonic porosity logs. These M-N plots show that most of the data points fall within sandstone zones and only few data points indicate the presence of carbonates and dolomite (Fig. 12,13,14).

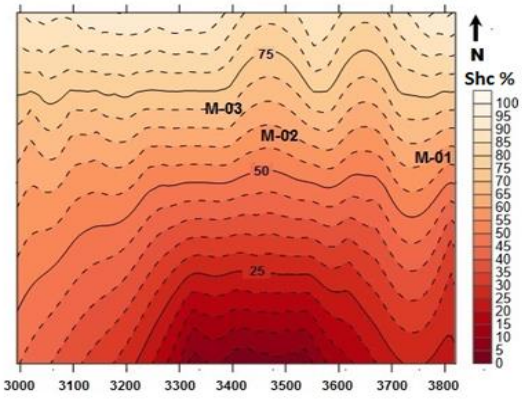

Fig. 11 Hydro carbon saturation distribution in Lower Goru Reservoir of Miano wells.

Hence, qualitative and quantitative interpretation of all petrophysical characteristics shows that with good porosity and permeability Sand B is clean and well sorted and has high hydrocarbon saturation in all three Miano wells. While, Sand C and D show low porosity and permeability with low hydrocarbon saturation and high intercalations of shale. However, more well logs

data is required for detailed study of Sand A, because Sand C has low hydrocarbon potential, thus unconventional recovery methods are recommended for future exploration. Well correlation study reveals that the Lower Goru reservoir is more productive in north to northeast region due to the thick sedimentation and high prolific hydrocarbon zone. It is also recommended that exploration and production wells should be drilled in the north to northeast of Miano field.

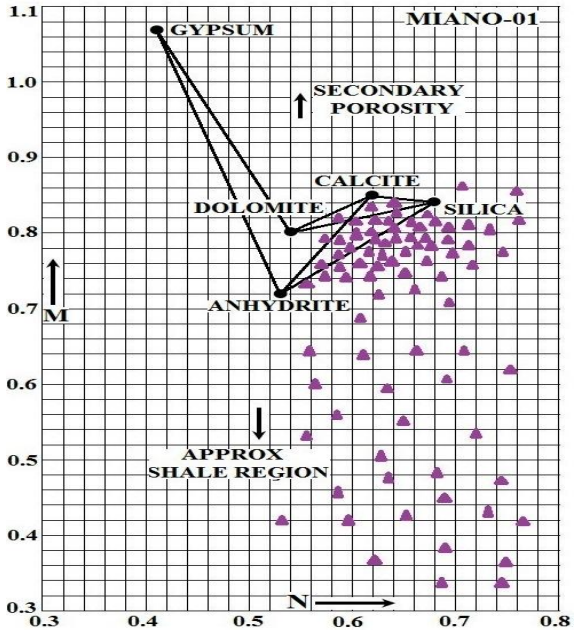

Fig. 12 MN Crossplot of Miano-1.

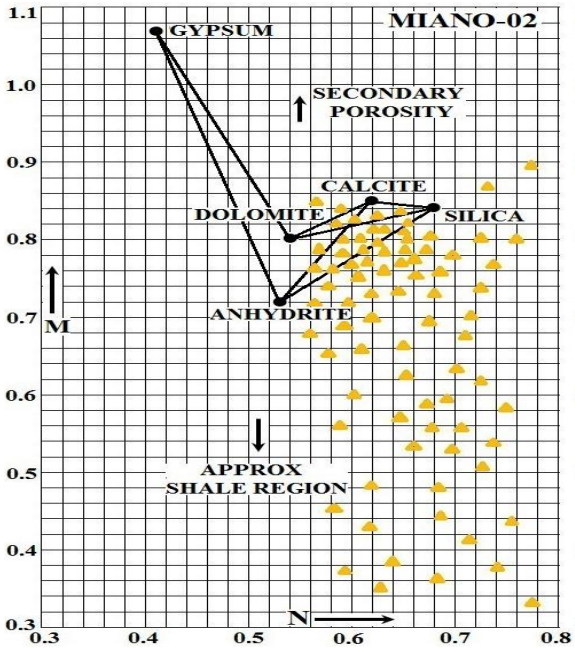

Fig. 13 MN Crossplot of Miano-2.

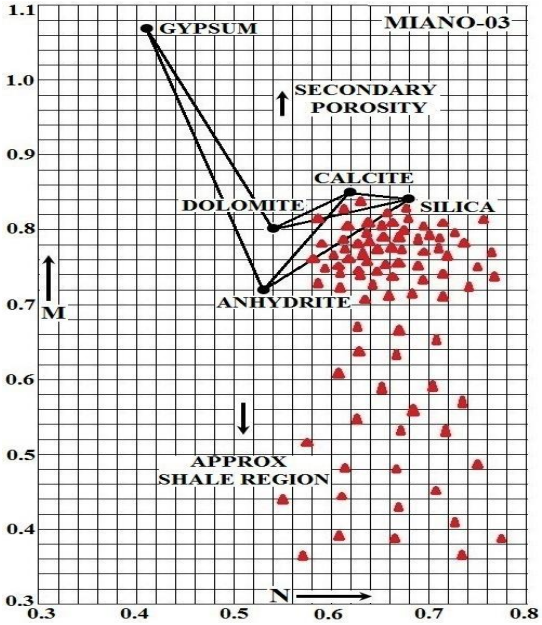

Fig. 14 MN Cross plot of Miano-3.

Conclusion

The petrophysical well log study of Miano 1, 2 and 3 wells showed that Sand B is a promising hydrocarbon bearing zone with 77%-80% hydrocarbon saturation, 19%-22% effective porosity, 798mD-847mD permeability and 19%-22% water saturation. The thickness of the Lower Goru reservoir increased from north to northeast direction with good reservoir characteristics and hydrocarbon prospects, while the M-N plots reveal that sandstone is a dominant component of the reservoir with shale and carbonate intercalations. Instead of dispersed shale, inter-bedded laminar shale is present within the Lower Goru reservoir sand, which drastically has caused reduction in porosity and has increased the water saturation. Sand A showed good reservoir characteristics, however better logs data is required for a detailed study for future prospects.

Declaration of Competing Interest

This study aims no conflict of interest to declare.

Acknowledgment

Directorate General of Petroleum Concession (DGPC) and Land Mark Graphics (LMKR) are highly acknowledged for providing the petrophysical well logging data to use for this research study.

References

Abbas, A., Zhu, H., Anees, A., Ashraf, U., Akhtar, N. (2019). An Integrated seismic interpretation, 2d

modeling along with petrophysical and seismic attribute analysis to decipher the hydrocarbon potential of Missakeswal area, Pakistan. *Int. J. Geol. Geophys.,* **8**(1), 455-467

Ahmed, N., Fink, P., Sturrock, S., Mahmood, T., Ibrahim, M. (2004). Sequence stratigraphy as predictive tool in Lower Goru Fairway, Lower and Middle Indus Platform, Pakistan. Pakistan Association of Petroleum Geoscientist (PAPG), Annual Technical Conference (ATC), 85–104.

Ahmed, Q., Khan, S. M., Masood, F., Jadoon, K. A. I., Akram, N. (2013). Mesozoic structural architecture of the Middle Indus Basin, Pakistan-Control and implications. *Int. J. Geos.*, **8**(4), 379-392.

Alabi, O. O., Sedara, S. O. (2016). Evaluation and accurate estimation from petrophysical parameters of a reservoir. *Int. Am. J. Env. Eng. Sci.*, **3**(2), 68-74.

Anees, A., Shi, W., Ashfra, U., Xu, Q. (2019). Channel identification using 3D seismic attributes and well logging in lower Shihezi Formation of Hangjinqi area, northern Ordos Basin, China. *Int. J. Appl. Geophys.*, **163**, 139–150.

Anees, A., Zhang, H., Ashraf, U., Wang, R., Liu, K., Mangi, N. H., Jiang, R., Zhang, X., Liu, Q., Tan, S., Shi, W. (2022). Identification of favorable zones of gas accumulation via fault distribution and sedimentary facies: Insights from Hangjinqi area, Northern Ordos Basin. *Int. J. Front. Earth Sci.,* **9**, 1-16.

Archie, G. E. (1942). The electrical resistivity log as an aid in determining some reservoir characteristics. *Int. J. Petrol. Tech.*, **146**(1), 54–62.

Ashraf, U., Zhu, P., Anees, A., Abbas, A., Talib, A. M. (2016). Analysis of Balkassar area using velocity modeling and interpolation to affirm seismic interpretation, Upper Indus Basin. *Int. J. Geos.*, **6**(3), 78–91.

Asquith, B. G., Gibson, R. C. (1982). Basic well log analysis. AAPG Methods in Exploration. Tulsa. USA. Series, **3**, 7-30.

Asquith, G., Krygowski, D., Henderson, S., Hurley, N. (2004). Basic well log analysis. AAPG Methods in Exploration. Tulsa. USA. Series **16,** 240–244.

Berger, A., Gier, S., Krois, P. (2009). Porosity-preserving chlorite cements in shallow–marine volcanic clastic sandstones: Evidence of the Sawan gas field, Pakistan. *AAPG Bulletin,* **9** (5), 595–615.

Cai, J., Wei, W., Hu, X., Wood, A. D. (2017). Electrical conductivity models in saturated porous media: a review. *Int. J. Earth Sci.*, **171**, 419–433.

Coats, G. R., Dumanoir, J. L. (1974). A new approach to improved log-derived permeability. SPWLA 14th annual logging symposium, Louisiana. USA. Paper No. SPWLA-1973-R.

Cosentino, L., Cheadle, A. B. (2001). Integrate reservoir study. *Bulletin of Canadian Petroleum Geology*, **51**(2), 209-211.

Jiang, R., Zhao, L., Xu, A., Ashraf, U. (2021). Sweet spots prediction through fracture genesis using multi-scale geological and geophysical data in the karst reservoirs of Cambrian Longwangmiao Carbonate Formation, Moxi-Gaoshiti area in Sichuan Basin, South China. *Int.J. Petrol. Explor. Prod. Tech.,* **12,** 1313-1328.

Kazmi, A. H., Jan, Q. M. (1997). Geology and Tectonics of Pakistan. Graphic Publishers, Karachi, Pakistan. 1st Edition, 528 pages.

Khan, N., Konate, A. A., Zhu, P. (2013). Integrated geophysical study of the Lower Indus Platform Basin Area of Pakistan. *Int. J. Geos.,* **4** (9), 1242-1247.

Krois, P., Mahmood, T., Milan, G. (1998). Miano field, Pakistan, a case history of model driven exploration. PAPG., Pakistan Petroleum Convention, Islamabad, Article, 90145.

Larionov, V. V. (1969). Borehole radiometry, basic well log analysis, using log-derived values of water saturation and porosity, trans. SPWLA Ann. Logging Symp. Paper, **10,** 26 pages.

Leveaux, J., Poupon, A. (1971). Evaluation of water saturation in shaly formations. Log Analyst SPWLA 12th Annual Logging Symposium, Dallas, Texas, Paper No. SPWLA-1971-O.

McPhee, C. A. Enzendorfer, C.K. (2004). Sand management solutions for high-rate gas wells, Sawan field, Pakistan. SPE International Symposium and Exhibition on Formation Damage Control. Lafayette, Louisiana, Paper No. SPE-86535-MS.

Patzek, K., Wilt, M., Hoversten, M. G. (2000). Using cross-hole electromagnetics (EM) for reservoir characterization and waterflood monitoring. SPE Permian Basin Oil and Gas Recovery Conference, Midland, Texas, Paper No. SPE-59529-MS

Powell, C.M., Dejong, K., Farah, A. (1979). Spectacular Tectonic history of Pakistan and its surrounding. geological survey of Pakistan, Quetta, 5-24.

Qadri, N. V., Shuaib, S. M. (1995). Hydrocarbon prospects of southern Indus Basin, Pakistan. *AAPPG Bulletin,* **70**(6), 730-747.

Raza, H.A. and Ahmed, R. (1990) Hydrocarbon Potential of Pakistan. *Journal of Canada Pakistan Cooperation,* **4**, 9-27.

Schlumberger, (1989). Log interpretation principles/applications manual. Schlumberger Educational Services, Houston, USA. 117 pages.

Iqbal, M. W. A; Shah, S. M. I (1980). A Guide to the Stratigraphy of Pakistan. Geological Survey of Pakistan. **53,** 40 pages.

Shepherd, M. (2009). Locating the remaining hydrocarbons. Oil field production geology. *AAPG*, **91,** 209 pages.

Timur, A. (1968). An investigation of permeability, porosity, and residual water saturation relationships for sandstone reservoirs. The Log Analyst, Paper No. SPWLA-1968-vIXn4a2.

Wandrey, J. C., Law, E. B., Shah, A. H. (2004). Sembar Goru/Ghazij composite total petroleum system, Indus and Sulaiman-Kirthar geologic provinces, Pakistan and India, *USGS Bulletin.*, 2004. Series. 2208, Chap. C., Version 1, 29 pages.

Whiteman, A. J. (1982). Nigera, its petroleum geology, resources and potentials. Graham & Trotman, **2**, 394 pages.

Wyllie, J. R. M., Gregory, R. A., Gardner, W. L. (1956). Elastic wave velocities in heterogeneous and porous media. Geophysicists, Tulsa, OK, United States, **21**(1), 41–70.

Wyllie, J. R. M., Rose, D. W. (1950). Some theoretical considerations related to the quantitative evaluation of the physical characterization of reservoir rock from electric log data. *J. Pet. Technol.* Paper No. SPE-950105-GW, **2** (4), 105–118.